Robust and Stable Hybrid Fuzzy Control of a Pendulum-Cart System with Particle Swarm Optimization

Yeong-Hwa Chang, C. W. Chang, W. S. Chan, J. S. Taur, and C. W. Tao

Abstract

In this paper, a hybrid fuzzy controller with a real-time particle swarm optimization algorithm (PSO) is presented to swing up and to stabilize the pendulum-cart system. The designed PSO with a re-start mechanism is particularly suitable for dynamic environments and its feasibility is evaluated using the typical dynamic functions. The modified particle swarm optimization is performed to on-line tune the parameters of hybrid fuzzy controllers. Also, the stability of the control system is discussed for the PSO optimized stable fuzzy control system. Simulation results, compared to conventional fuzzy control, illustrate that the proposed optimization-based control scheme can provide better control performance subject to extra disturbances.

Keywords: Particle swarm optimization, fuzzy control, pendulum-cart system, dynamic function, stability.

1. Introduction

Particle swarm optimization (PSO) algorithm is a population-based evolutionary computation method, inspired to mathematically simulate the social behavior of bird flocking and fish schooling. Similar to genetic algorithm (GA), PSO is also initiated with a population of candidates that are randomly moved in a multidimensional search space [1-2]. However, GA saves only the better generations, thus it may easily lead to local optima rather than the global optimum, and the operating on dynamic data sets is difficult [3-4].

Recently, PSO has been successfully applied to many fields of interest. In [1], robot systems are optimally voice-controlled by a PSO algorithm. In [3], [5-7], PSO algorithms are applied to the optimal design of power distribution, buck-boost transformer, and voltage regulation controller. The rule-based delay proportion adjustment for proportional differentiated services is optimized with an extensional PSO algorithm [8]. In [9-10], PSO-optimized algorithms can be applied to train the parameters of some neural networks. PSO algorithm can also be utilized for the image reconstruction problem in digital image processing [11-12].

Although the applications with PSO algorithms have been found in many research areas, PSO optimization for real-time adjustment has not been fully discussed yet. It is motivated to propose a real-time PSO algorithm so that the enhanced searching ability can be affordable for dynamic environments. To successfully perform the PSO in a dynamically varying environment, two mechanisms are required. First, it is required to provide a detecting ability while the change of environment occurs. Once the searching space is varied, PSO must be adaptively tuned to meet the new dynamical characteristics. Second, the ability to re-start a new search is desired, especially in a varying space [3], [13-14]. In the literature, the re-start mechanism is to have all of the parameters and particle positions initiated again and to re-start the PSO algorithm. This re-start mechanism is not allowed with some of the on-line real time application such as the system control. When the parameters of the controller (particle positions) suddenly initiated with random values, the performance of the control system will be degraded, moreover, the system maybe become even unstable.

It is known that the pendulum-cart system is highly sensitive to the disturbance. With the characteristics of fuzzy techniques to reduce the influence of the disturbances, fuzzy controllers would be considered for stabilizing the pendulum-cart system. However, the parameters in the fuzzy mechanism are difficult to be determined. Several learning techniques have been applied to learn the parameters in the fuzzy techniques. Among these learning techniques, PSO is better than GA for the on-line tuning. Thus, in this paper, a hybrid fuzzy controller is presented for the swing-up and balance of the pendulum-cart system with the RT-PSO for the parameter optimization under the external disturbance. The feasibility of the RT-PSO scheme is evaluated using some dynamic functions.

To indicate the effectiveness of the designed fuzzy controller with the RT-PSO algorithm, the stability of the hybrid fuzzy controlled pendulum-cart system is discussed in this paper. With the nonlinear pendulum-cart system equally expressed as a T-S fuzzy model in all the fuzzy regions, the parallel distribution singleton

Corresponding Author: C.-W. Tao is with the Department of Electrical Engineering, National Ilan University, Ilan Taiwan
E-mail: cwtao@niu.edu.tw
Manuscript received May 2008; revised July 2008; accepted Dec. 2008.

control (PDSC) is utilized and the stability is guaranteed according to the Lyapunov's Theorem [15]-[19].

This paper is organized as follows. Section 2 presents the real-time PSO algorithm. The model of pendulum-cart system and the proposed approach are described in Section 3. The stability of the control system is addressed in Section 4. In Section 5, simulation results compared to the results using the fuzzy control without on-line parameter tuning are provided. The concluding remarks are given in Section 6.

2. Real-Time PSO Algorithm

A. *Conventional PSOs*

In the PSO algorithms, each particle can be viewed as a distinct individual. To achieve a better fitness, every particle updates its positions according to the history velocity and memory of its own. The velocity of each particle is updated based on its current best solution and the current global best solution in swarm. PSO is inherited with random parameters that provide the ability to avoid local optimal solution with less concern of staring position. Let the search space be a *j*-dimensional space. The *j*-th dimensional position, velocity, personal best solution and global best solution for the *i*-th particle are denoted as P_i^j, V_i^j, $Pbest_i^j$ and $Gbest^j$, respectively. The adaptive particle swarm optimization (APSO) algorithm can be modeled as two iterative equations [11]:

$$V_i^j(t+1) = w \cdot V_i^j(t) + c_1 \cdot r_1 \cdot \left(Pbest_i^j(t) - P_i^j(t)\right) + c_2 \cdot r_2 \cdot \left(Gbest^j(t) - P_i^j(t)\right) \quad (1)$$

$$P_i^j(t+1) = P_i^j(t) + V_i^j(t+1) \quad (2)$$

where t is the iteration index, w is the inertia weight of the particle velocity, r_1 and r_2 are the uniformly distributed random variables in the range of [0,1], c_1 and c_2 are the acceleration coefficients to move the particle toward the best solution. As indicated in [3], the velocities of particles are limited to be in a range of $[-V_{\max}, V_{\max}]$, where $V_{\max}$ is selected to damp the trajectory oscillation and to have the optimal solution. For simplicity, $P_i^j(t)$ and $V_i^j(t)$ are simply denoted as $P_i(t)$ and $V_i(t)$ in the rest of this paper.

In general, if a small value of w is adopted, the particle will converge to the optimal solution within a small number of iterations. Otherwise, the search range of particles will be increased with a larger value of w. When the acceleration coefficients $c_1 > c_2$, each particle intends to move toward the personal best solution. On the contrary, the particles in one group would move toward the global best solution instead. When particles are with the same personal best solution and global best solution, the random variables r_1 and r_2 are utilized to strengthen the search diversity. It is noticed that both the simple PSO and APSO are typically utilized off-line for stochastic optimization of concern. For complex systems with significant dynamic characteristics, off-line tuning methods seem to be not adequate.

B. *Real-Time PSO (RT-PSO)*

Under the circumstance of variations existed in system dynamics, if the updated optimal fitness value is less than the previous one, conventional PSOs may mislead to an incorrect searching area. In this paper, a so-called sentry particle (*Ps*) is added to monitor the change of environment. The basic idea to detect the variations of system dynamics is explained in the following. In the *t*-iteration, the *Pbest* and associated fitness value of a randomly chosen particle are assigned to the sentry particle, denoted as $Ps = Pbest$ and $F = f(Pbest)$. In the next iteration, the fitness value of *Ps* is calculated again according to the current environment, denoted as $\tilde{f}(Ps)$. Note that when the variations of system dynamics are possible, $\tilde{f}$ might not be equal to *f*. If $f(Ps) \neq F$, it can be considered that the environment change happens. Once the variations of system dynamics are detected, the re-start mechanism is performed. Unlike the re-start mechanism in the literature to have all of the parameters and particle positions initiated again and to re-start the PSO algorithm, the proposed re-start mechanism only deletes the personal best value of each particle and adopts the following equation to update the velocity of each particle,

$$V_i^j(t+1) = \kappa \cdot rand \cdot V_{\max}^j \quad (3)$$

where κ is some constant, *rand* is a random number in [-1, 1] and $V_{\max}^j$ is the velocity limit.

Furthermore, if the updated velocity is small enough, i.e. $|V_i^j| \leq \varepsilon$, it means that a certain optimum is approached. To avoid being trapped in the local optima, the re-start mechanism needs to start working again such that the searching capability should be enhanced. In order to effectively implement the proposed RT-PSO algorithm, some assumptions are required. Considering the real-time implementation, a reasonable space size for the parameter searching is required. In addition, the dynamic system with the RT-PSO algorithm is required to have smooth characteristics. Otherwise, the computation cost will be too high to be affordable. The scenario of the RT-PSO algorithm is summarized as the Fig. 1.

C. *RT-PSO for Dynamic Objective Functions*

A dynamic objective function is defined as follows

$$f(x) = H_{\max} - \frac{H}{1 + 0.01 \cdot \sum_{j=1}^{10} (x^j - X^j)^2} \quad (4)$$

$$H = \begin{cases} H_0 & t < 2500 \\ H_0 + 50 \cdot rand & t = 2500 \end{cases}$$

$$X^j = \begin{cases} X_0^j & t < 2500 \\ X_0^j + rand & t = 2500 \end{cases}$$

$$H_0 = 50,\quad X_0^j = rand\,,\quad H_{\max} = \max(H)$$

The associated distribution of fitness values is shown in Fig. 2. Obviously, the optima are varied due to different setting conditions. In Fig. 3, it can be seen that in the first 2500 iterations, both APSO and RT-PSO give the similar convergence tendencies of fitness values. However, upon the environmental change, the APSO optimized fitness value jumps high and keeps the value afterward. It means that the APSO fails to search for the new optimal solution due to the change of environment. On the other hand, the RT-PSO can effectively decrease the fitness value and converge to the optimal solution.

START
Step 1 (initialization)
Initialize the population
Randomly select the *Ps* from particles in the initialized population
Let $F = f(Pbest)$
Step 2
For *i* = 1 to number of particles $f(P_i)$
Evaluate the fitness
Update $Pbest_i$ and $Gbest$
For *j* = 1 to dimension
Update each particle's velocity according to (1)
If $|V_i^j| \le \varepsilon$
Re-start the velocity according to (3)
If $|V_i^j| > V_{\max}^j$
$V_i^j = \mathrm{sgn}(V_i^j) \cdot V_{\max}^j$
Update each particle's position according to (2)
Increase *j*
Increase *i*
Step 3
If $f(Ps) \ne F$ {
Clear the memory for all particles
Re-start velocities for all particles according to (3)}
Step 4
Randomly select one *Pbest* from all *Pbest*s to be the Sentry particle *Ps*
Let $Ps = Pbest$; $F = f(Pbest)$
Step 5
If stop criterion is reached then **STOP**
else Goto Step 2

Fig. 1. Pseudo code of RT-PSO.

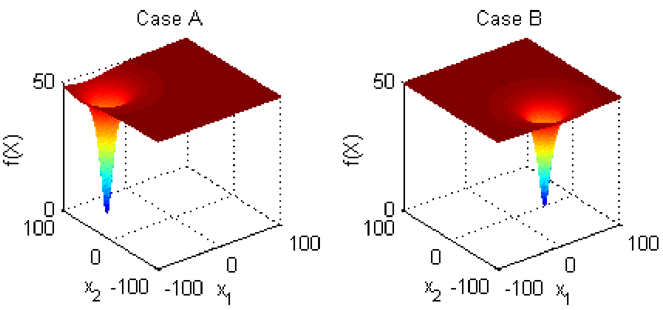

Fig. 2. Cross-section view of the dynamic function: $t < 2500$ (left), $t \ge 2500$ (right).

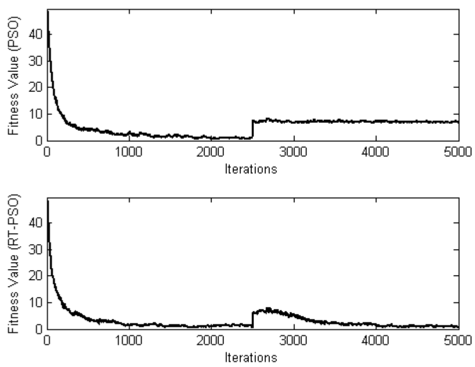

Fig. 3. Fitness values of dynamic objective functions via different PSO algorithms: APSO (top), RT-PSO (bottom).

3. RT-PSO Optimized Fuzzy Control of Pendulum-Cart System

A. *System Model of Pendulum-Cart System*

The pendulum-cart system has been a well known system to verify control strategies in literature. In this paper, a hybrid fuzzy controller is designed to make the pendulum swing up and balance at the upright position. The state vector $x = [x_1 \ \ x_2 \ \ x_3 \ \ x_4]^T$ is defined with x_1, x_2, x_3, and x_4 being the position of the cart, the angle of the pendulum, the velocity of the cart, and the angular velocity of the pendulum, respectively. The state equations of pendulum-cart system are described as follows [15]:

$$\begin{aligned} \dot{x}_1 &= x_3 \\ \dot{x}_2 &= x_4 \\ \dot{x}_3 &= \frac{a\left(U - T_c - \mu \cdot x_4^2 \sin x_2\right) + l \cdot \cos x_2 \left(\mu \cdot g \cdot \sin x_2 - f_p \cdot x_4\right)}{J + \mu \cdot l \cdot \sin^2 x_2} \\ \dot{x}_4 &= \frac{l \cdot \cos x_2 \left(U - T_c - T_d - \mu \cdot x_4^2 \cdot \sin x_2\right) + \mu \cdot g \cdot \sin x_2 - f_p \cdot x_4}{J + \mu \cdot l \cdot \sin^2 x_2} \end{aligned} \tag{5}$$

where *U* is the control command, T_c is the friction force, *l* is the distance between the rotation axis and the center of the pendulum mass, *g* is the gravity acceleration constant, f_p is the friction constant of the pendulum, *J* is the inertia of the pendulum, and T_d is the disturbance.

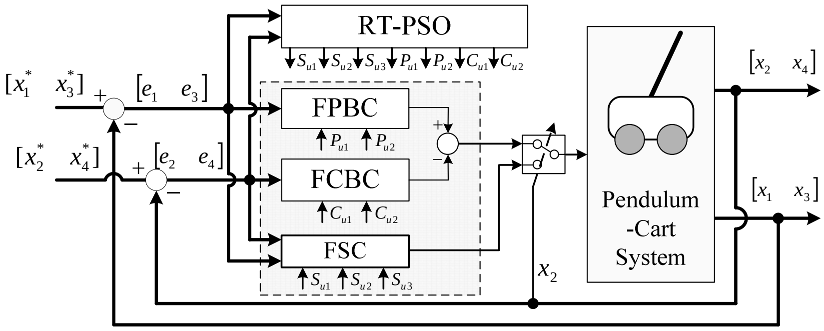

Fig. 4. The structure of the pendulum-cart control system with RT-PSO.

Moreover $a = l^2 + J/(m_c + m_p)$ and $\mu = l \cdot (m_c + m_p)$ with m_c and m_p being the mass of the cart and the pendulum. It is noted that the mass of the pendulum is not uniformly distributed and the friction between the cart and the track is nonlinear and approximated by the following piecewise linear and quadratic equations [15]:

$$\begin{cases} T_c = \dfrac{(Y_c - F_c)}{X_c} x_3 + F_c & , \ |x_3| \geq X_c \\ T_c = \dfrac{(F_s - Y_c)}{X_c^2} x_3^2 - \dfrac{2(F_s - Y_c)}{X_c} x_3 + F_s & , \ V_{DZ} \leq |x_3| \leq X_c \\ T_c = \dfrac{F_s}{V_{DZ}} x_3 & , \ |x_3| < V_{DZ} \end{cases} \quad (6)$$

where F_s and F_c represent the static and the dynamic friction, X_c is the starting cart velocity for the linear zone, Y_c is the friction value at the velocity X_c, and V_{DZ} is the dead zone of the cart velocity.

B. *RT-PSO Fuzzy Swing-Up and Balance Controllers*

The schematic diagram of the pendulum-cart control system with RT-PSO is shown in Fig. 4, where x_k^* is the command of x_k and $e_k = x_k^* - x_k$ is the error of state variable, k=1,…,4. To simplify the control of the pendulum-cart system, the pendulum-cart system is decoupled into the pendulum and the cart subsystems. Two fuzzy control strategies are utilized to swing up the pendulum and to balance the pendulum and the cart at the designated position. The diagram for the pendulum states is shown in Fig. 5.

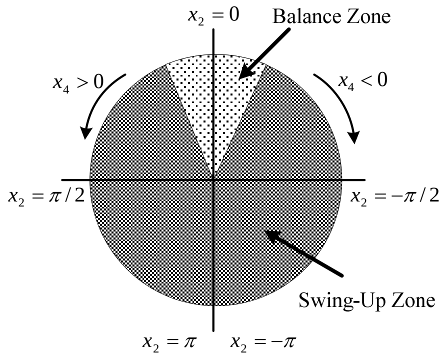

Fig. 5. The illustration diagram of the pendulum state.

Let $x_2 = 0$ be defined as the vertical upright position for the pendulum. The balance controller will not be executed unless the pendulum is in the balance zone, $|x_2| \leq \pi/10$. The control strategy is to take the fuzzy swing-up controller to upswing the pendulum into the balance zone and then to utilize the fuzzy balance controller to complete the balance control of the pendulum and the cart. The proposed RT-PSO optimized control scheme contains a fuzzy swing-up controller (FSC), a fuzzy pendulum-balance controller (FPBC), a fuzzy cart balance controller (FCBC), and the RT-PSO tuning mechanism.

1) Fuzzy Swing-up Controller (FSC)

The fuzzy swing-up controller aims to accumulate enough system energy to allow the pendulum to swing-up into the balance zone. Also, it is required to suppress the position change of cart. With these control goals considered, $e_2 = x_2^* - x_2$ and $e_3 \cdot \mathrm{sgn}(e_1)$ are designed as the inputs of the fuzzy swing-up controller, where sgn is a standard sign function.

It can be seen that if the output of the fuzzy swing-up controller makes the cart move to the right, the pendulum swings counterclockwise when $|x_2| < \pi/2$ or clockwise when $|x_2| \geq \pi/2$. To suppress the position error of the cart, the fuzzy swing-up controller drives the cart to the right (left) when the cart is on the left hand side (right hand side) with the negative (positive) velocity. Based on the mentioned control strategies above, the membership functions (MFs) of the fuzzy swing-up controller is constructed as in Fig. 6, where I_{s1} and I_{s2} are antecedent variables, and O_s is the consequent variable.

2) Fuzzy Balance Controllers (FPBC and FCBC)

Approaching into the balance zone, the controller switches from the swing-up control to the balance control. The goal of the balance control is to stabilize the pendulum at the position $x_2 = 0$ and to keep the position of cart at $x_1 = 0$ as well. The pendulum angle and the angular velocity are used as inputs of FPBC for the pendulum subsystem. The FPBC is designed to balance the pendulum to its upright position. Similarly, the cart position and the cart velocity are designed as the input variables of the fuzzy controller FCBC. In Figs. 6 and 7, the input and output membership functions of FPBC and FCBC are indicated, where $I_P = [I_{Pq}\ I_{Pw}]$ and $I_C = [I_{Cx}\ I_{Cv}]$ represent the input vectors of FPBC and FCBC, respectively. The O_P and O_C are denoted as the output vectors of FPBC and FCBC, respectively. For the entire pendulum-cart system, the integrated output is considered as $O_B = O_P - O_C$.

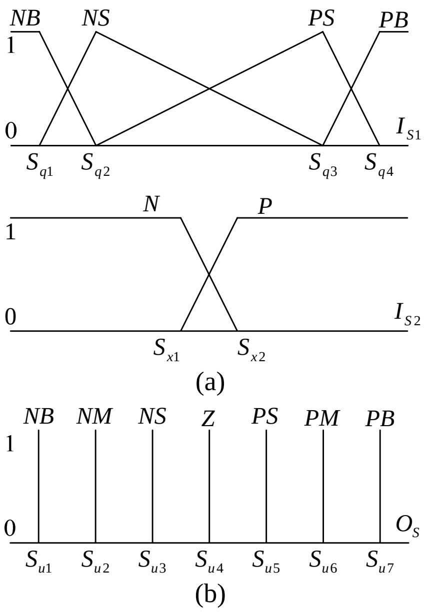

Fig. 6. The MFs of swing-up strategy: (a) input membership functions, (b) output membership functions.

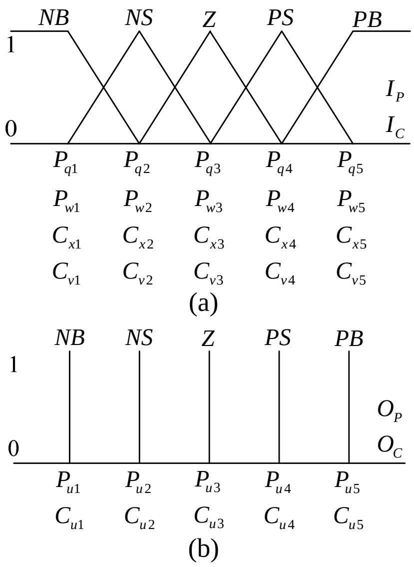

Fig. 7. The MFs of balance strategy: (a) input membership function, (b) output membership function.

According to the aforementioned discussion, the balance controller is applied when the pendulum is in the balance zone. Otherwise, the swing-up control strategy is adopted to accumulate system energy. Namely, the control scenario is switched between the balance and swing-up control strategies according to the pendulum angle, i.e.

$$U = \begin{cases} O_S, & if\ x_2 > \pi/10 \\ O_B, & if\ x_2 \le \pi/10 \end{cases} \tag{7}$$

where U is the output of the controller for the pendulum-cart system.

4. Stability of the Fuzzy Control

Takagi-Sugeno (T-S) fuzzy model is described by fuzzy IF-THEN rules, which represent local linear input-output relations of the nonlinear system. It notes that the nonlinear system is approximated by a set of linear subsystems. Let r be the number of fuzzy rules. The format of the i-th rule is as following:

Model Rule i :

IF x_1 is M_{i1} and … and x_n is M_{in}

THEN $\dot{x} = A_i x + B_i u$, $i = 1,2,...,r$ (8)

where M_{iq} with the corresponding membership function $M_{iq}(x_q)$ is a fuzzy set in the rule i, $q = 1,2,...,n$. $x \in R^n$ is the state vector, $u \in R^m$ is the control input vector, A_i and B_i are constant coefficient matrices, and $A_i \in R^{n\times n}$, $B_i \in R^{n\times m}$. Based on the standard fuzzy inference principle, the sum-product inference and the centroid defuzzification, the state equation of the system with T-S fuzzy model is described by

$$\dot{x} = \frac{\sum_{i=1}^{r} \omega_i(x)\{A_i x + B_i u\}}{\sum_{i=1}^{r} \omega_i(x)} = \sum_{i=1}^{r} h_i(x)\{A_i x + B_i u\} \tag{9}$$

where $\omega_i(x) = \prod_{k=1}^{n} M_{ik}(x_k)$ is the weight of the i-th rule, $M_{ik}(x_k)$ is the grade of membership of x_k in M_{ik}, $h_i(x) = \omega_i(x) / \sum_{i=1}^{r} \omega_i(x)$, $h_i(x) \in [0\ \ 1]$, and $\sum_{i=1}^{r} h_i(x) = 1$.

Based on the parallel distributed compensation (PDC) technique [16], the T-S fuzzy controller can be represented as

Control Rule i :

IF x_1 is M_{i1} and x_i is M_{in}

THEN $u = -F_i x$, $i = 1,2,...,r$ (10)

where F_i is the local feedback gain of the fuzzy controller. The global control action would be

$$u = -\sum_{i=1}^{r} h_i(x) F_i x,\ \ i = 1,2,...,r\ . \tag{11}$$

Substituting (11) into (9), the state equation of a closed-loop fuzzy control system with the T-S fuzzy model and the PDC controller becomes

$$\dot{x} = \sum_{i=1}^{r}\sum_{j=1}^{r} h_i(x)h_j(x)\{A_i - B_i F_j\}x \tag{12}$$

Theorem 1[16]: The nonlinear system approximated by a T-S fuzzy model with the PDC in (12) is globally asymptotically stable if there exists a common symmetric and positive definite matrix ***P*** such that

$$G_{ii}^T P + PG_{ii} < 0\,, \tag{13}$$

$$G_{ij}^T P + PG_{ij} < 0\,, \tag{14}$$

where

$$G_{ii} = A_i - B_i F_i\,, \tag{15}$$

$$G_{ij} = \frac{(A_i - B_i F_j) + (A_j - B_j F_i)}{2}. \tag{16}$$

To have a T-S fuzzy model with the PDC be globally stable, the feedback gain F_i needs to be determined to satisfy the conditions in (13)-(16).

Theorem 2: Compared to the Theorem 1 above, if the new feedback gain, F_i', $F_i' = \alpha F_i$, $0 \le \alpha < 1$, is selected, and there exists a common symmetric and positive definite matrix ***P*** such that

$$G_{ii}^T P + PG_{ii} < 0\,, \tag{17}$$

$$G_{ij}^T P + PG_{ij} < 0\,, \tag{18}$$

$$H_{ii}{}^T P + PH_{ii} < 0\,, \tag{19}$$

$$H_{ij}{}^T P + PH_{ij} < 0\,, \tag{20}$$

with $H_{ii} = B_i F_i$, $H_{ij} = \dfrac{B_i F_j + B_j F_i}{2}$

then the control system is globally asymptotically stable.

Proof: From Theorem 1, the closed-loop nonlinear system is stable with the derived feedback gain F_i. For the new feedback gains $F_i', F_i' = \alpha F_i$, G_{ii}' and G_{ij}', can be obtained as

$$G_{ii}' = A_i - \alpha B_i F_i \tag{21}$$

$$G_{ij}' = \frac{\{A_i - \alpha B_i F_j\} + \{A_j - \alpha B_j F_i\}}{2}. \tag{22}$$

From (21), it gives that

$$\begin{aligned}
&G_{ii}'^T P + PG_{ii}' \\
&= \{A_i - \alpha B_i F_i\}^T P + P\{A_i - \alpha B_i F_i\} \\
&= \{A_i - B_i F_i\}^T P + P\{A_i - B_i F_i\} + (1-\alpha)\left(\{PB_i F_i\}^T + \{PB_i F_i\}\right) \\
&= G_{ii}^T P + PG_{ii} + (1-\alpha)\left\{H_{ii}{}^T P + PH_{ii}\right\}
\end{aligned}$$

By the stability conditions in Theorem 2,

$$G_{ii}'^T P + PG_{ii}' < 0 \tag{23}$$

can be derived. Similarly, from (22) we can find that

$$\begin{aligned}
&G_{ij}'^T P + PG_{ij}' \\
&= \left\{\frac{\{A_i - \alpha B_i F_j\} + \{A_j - \alpha B_j F_i\}}{2}\right\}^T P \\
&\quad + P\left\{\frac{\{A_i - \alpha B_i F_j\} + \{A_j - \alpha B_j F_i\}}{2}\right\} \\
&= G_{ij}^T P + PG_{ij} + \left\{\frac{(1-\alpha)\left(\{B_i F_j\} + \{B_j F_i\}\right)}{2}\right\}^T P \\
&\quad + P\left\{\frac{(1-\alpha)\left(\{B_i F_j\} + \{B_j F_i\}\right)}{2}\right\} \\
&= G_{ij}^T P + PG_{ij} + (1-\alpha)\left\{H_{ij}^T P + PH_{ij}\right\}
\end{aligned}$$

Again if the conditions (19)-(20) in Theorem 2 are satisfied,

$$G_{ij}'^T P + PG_{ij}' < 0 \tag{24}$$

According to Theorem 1, if equation (23) and (24) are satisfied, the T-S fuzzy model with the PDC using the new feedback gain, F_i', is globally asymptotically stable. ♦

The Theorem 2 can be extend to the Mamdani type fuzzy controller. Let Mamdani type fuzzy output u_F be proportioned to the PDC controller output u_{TS},

$$u_F = k\,\mathrm{sgn}(u_{TS}) = -k\,\mathrm{sgn}(Fx) = -\frac{k}{\|Fx\|}Fx = -\alpha Fx \tag{25}$$

where $\alpha = k/\|Fx\|$, k is the output gain of the Mamdani type fuzzy controller. From the Theorem 2, we can know that the Mamdani type fuzzy controller is stable if k satisfies follow condition

$$0 \le k < \min(\|Fx\|) \tag{26}$$

with x in the corresponding fuzzy region.

For example, let the fuzzy rules with the input membership functions ($M_1(x_1)$, $M_2(x_2)$) of a 2-dimension fuzzy controller be showed as Fig.8. The singleton output membership function $M(out)$ is shown in Fig.9. It can be seen that each of the input variables has five fuzzy sets, negative big (NB), negative small (NS), zero (Z), positive small (PS), and positive big (PB). The fuzzy IF-THEN rules are expressed as

$$R_j: \text{IF } x_1 \text{ is } M_{j1} \text{ and } x_2 \text{ is } M_{j2}, \quad \text{THEN } u_F \text{ is } G_j, \tag{27}$$

where x_i, $i = 1,2$, are state variables, M_{j1}, M_{j2}, and G_j, $j = 1,2...,25$, are the corresponding fuzzy sets, u_F is the control action. Although the Mamdami fuzzy rules are in general for the design of fuzzy controllers, that is, the nonlinear system function $\dot{x} = f(x,u)$ is not expressed in the Mamdami fuzzy rules, it implicitly indicate that the nonlinear system function is the same for all the fuzzy regions. Thus, it might be reasonable to have the Mamdami fuzzy control system with rules as

R_j : IF x_1 is M_{j1} and x_2 is M_{j2},

THEN $\dot{x} = f(x,u)$ with $u = u_F$ being G_j,

where the nonlinear system function $\dot{x} = f(x,u)$ is the same for all the rules. With the nonlinear system being equivalently represented as a T-S modeled system in each fuzzy region described in the corresponding fuzzy rule, the Mamdani type fuzzy control system can be considered as a T-S fuzzy control system with

R_j : IF x_1 is M_{j1} and x_2 is M_{j2},

THEN if x_1 is M_{i1} and x_2 is M_{i2}

then $\dot{x} = A_i x + B_i u$, $i = 1,2,...,r$ with $u = u_F$

being G_j.

Note that the T-S models in all the regions are the same and exactly equal to the original nonlinear system. If there exists a diagonal line (as indicated in Fig. 8) on the input space which is defined as

$$L: c_1 x_1 + c_2 x_2 = 0,$$

then the feedback gain F can be determined as

$$F = [c_1 \quad c_2].$$

It is known that parameters c_1 and c_2 can be adjusted to have an effective feedback gain. From the Fig. 8, it can be seen that the singleton value k_j (see Fig. 9) of G_j is

$$k_j = -\beta_j \operatorname{sgn}(Fx)$$

for x in the corresponding fuzzy region. Thus, with the k_j proper designed to satisfy $0 \le \beta_j < \min(\|Fx\|)$, j=1,..5, the Mamdani type fuzzy control system can be globally stable according to Theorem 2.

Corollary 1: Based on the Theorem 2, the pendulum-cart system with FPBC and FCBC would be globally asymptotically stable if the singleton value k_j of G_j, j=1,..5, is designed as

$$k_j = -\beta_j \operatorname{sgn}(Fx)$$

where $0 \le \beta_j < \min(\|Fx\|)$ with x in the corresponding fuzzy region and if there exists a common symmetric and positive definite matrix $\boldsymbol{P}$ such that

$$G_{ii}^T P + P G_{ii} < 0, \tag{17}$$

$$G_{ij}^T P + P G_{ij} < 0, \tag{18}$$

$$H_{ii}{}^T P + P H_{ii} < 0, \tag{19}$$

$$H_{ij}{}^T P + P H_{ij} < 0, \tag{20}$$

with $H_{ii} = B_i F_i$, $H_{ij} = \dfrac{B_i F_j + B_j F_i}{2}$,

then the control system is globally asymptotically stable.

Proof: As in the explanation paragraphs above the Corollary 1. ♦

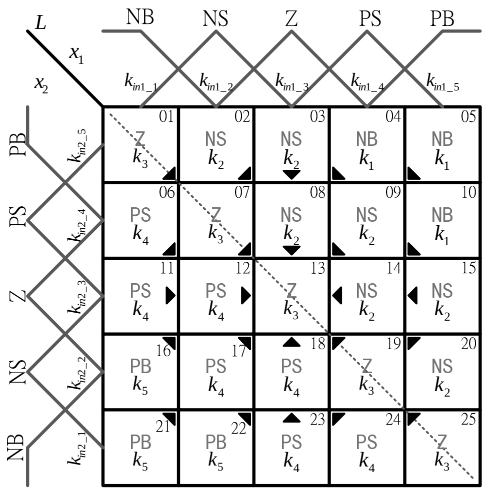

Fig. 8. The Mamdani type fuzzy rule table.

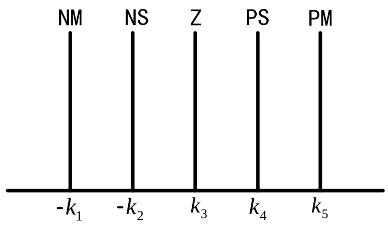

Fig. 9 The output membership function.

5. Simulation Results

For the pendulum-cart system, it can be decoupled to be two subsystems, pendulum subsystem and cart subsystem. The T-S model of cart subsystem can be illustrated as

Rule 1:

IF x_3 is M_1, THEN

$$\dot{x}_c = A_{c1} x_c + B_{c1} u$$

Rule 2:

IF x_3 is M_2, THEN

$$\dot{x}_c = A_{c2} x_c + B_{c2} u.$$

The membership functions $M_1(x_3)$ and $M_2(x_3)$ can be denoted as

$$M_1(x_3) = \frac{f_c - f_{c1}}{f_{c1} - f_{c2}},$$

$$M_2(x_3) = \frac{f_c - f_{c2}}{f_{c1} - f_{c2}}$$

where

$$f_c = \frac{a\left(-T_c - \mu \cdot x_4^2 \sin x_2\right) + l \cdot \cos x_2 \left(\mu \cdot g \cdot \sin x_2 - f_p \cdot x_4\right)}{J + \mu \cdot l \cdot \sin^2 x_2}$$

$$f_{c1} = a_{c1} x_3,$$

$$f_{c2} = a_{c2} x_3$$

with a_{c1} and a_{c2} are the coefficients which will appear in the system matrices A_{c1} and A_{c2} of the T-S model for the cart subsystem. Likewise, for the pendulum subsystem, the T-S model can be illustrated as

Rule 1:

IF x_2 is N_1, THEN

$$\dot{x}_p = A_{p1}x_p + B_{p1}u$$

Rule 2:

IF x_2 is N_2, THEN

$$\dot{x}_p = A_{p2}x_p + B_{p2}u$$

The membership functions of the pendulum subsystem, $N_1(x_2, x_4)$ and $N_2(x_2, x_4)$ are

$$N_1(x_2, x_4) = \frac{f_{pp} - f_{p1}}{f_{p1} - f_{p2}},$$

$$N_2(x_2, x_4) = \frac{f_{pp} - f_{p2}}{f_{p1} - f_{p2}}$$

where

$$f_{pp} = \frac{l\cos x_2\left(-T_c - T_d - \mu \cdot x_4^2 \cdot \sin x_2\right) + \mu g \sin x_2 - f_p \cdot x_4}{J + \mu l \sin^2 x_2}$$

$$f_{p1} = a_{p1}x_2,$$

$$f_{p2} = a_{p2}x_2.$$

The a_{p1} and a_{p2} are the parameters in the system matrices A_{p1} and A_{p2} of the T-S model for the pendulum subsystem. The matrices of the T-S modeled cart and pendulum subsystems can be obtained as

$$A_{c1} = \begin{bmatrix} 0 & 1 \\ 0 & 5 \end{bmatrix} \qquad B_{c1} = \begin{bmatrix} 0 \\ 0.87 \end{bmatrix}$$

$$A_{c2} = \begin{bmatrix} 0 & 1 \\ 0 & 3 \end{bmatrix} \qquad B_{c2} = \begin{bmatrix} 0 \\ 0.87 \end{bmatrix}$$

$$A_{p1} = \begin{bmatrix} 0 & 1 \\ 50 & 0 \end{bmatrix} \qquad B_{p1} = \begin{bmatrix} 0 \\ 3.65 \end{bmatrix}$$

$$A_{p2} = \begin{bmatrix} 0 & 1 \\ 10 & 0 \end{bmatrix} \qquad B_{p2} = \begin{bmatrix} 0 \\ 3.56 \end{bmatrix}$$

Using the MATLAB LMI toolbox and (17)-(20), the feedback gains and the associated positive definite matrix for each subsystem can be found as follows

$$F_p = \begin{bmatrix} -158.6 & -4.1 \end{bmatrix} \qquad F_c = \begin{bmatrix} 2.90 & 14.95 \end{bmatrix}$$

$$P_p = \begin{bmatrix} 148.05 & 3.86 \\ 3.86 & 0.37 \end{bmatrix} \qquad P_c = \begin{bmatrix} 2.69 & 6.47 \\ 6.47 & 24.25 \end{bmatrix}$$

Note that as the Mamdani type fuzzy controller described in the Section 4, the feedback gains for the T-S pendulum subsystems are required to be the same. Likewise, the feedback gains for the T-S cart subsystems are also required to be the same. Based on Theorem 2, it can be shown that the T-S fuzzy modeled pendulum-cart system is asymptotically stable with the Mamdani type fuzzy controller.

In order to make the system be robust to the disturbance, the RT-PSO is proposed to real-time adjust the parameters of the mentioned fuzzy controllers. The parameters of RT-PSO are given in Table 1. It is noted that the restrictions about the particle velocity and the allowable variation of the initial random range are considered to prevent system instability.

Table 1. The parameters of RT-PSO.

Parameters	Value
Number of particles (*n*)	5
Inertia weight (*w*)	0.8
Coefficient (c_1, c_2)	2, 2
Velocity limit ($V_{\max}$)	0.2*(Tuned Parameters)
Initially range of random search	[-0.1, 0.1]*(Tuned Parameters)

The settings of pendulum-car system are listed in Table 2. For simplicity, input and output membership functions are assumed to be symmetric. In this paper, from Fig. 4, the proposed RT-PSO is utilized to adjust the parameters of the output membership functions, i.e. S_{u1}, S_{u2}, S_{u3} in Fig.6(b) for the swing-up controller, P_{u1}, P_{u2} for the pendulum balance controller, and C_{u1}, C_{u2} for the cart position controller in Fig.7(b). According to the control goal of upswing and balance to have the guaranteed stability of the system, two fitness functions are respectively defined as follows

$$Fitness_{swing-up} = (1 - \exp(-|(m_p gl\cos(e_2) + \frac{1}{2}Jx_2^2) - m_p gl)|) \tag{28}$$

$$\begin{aligned} Fitness_{balance} = &(1 - \exp(-|e_2|)) \cdot (1 + \exp(-|e_4|)) \\ &+ (1 - \exp(-|e_1|)) \cdot (1 + \exp(-|e_3|)) \end{aligned} \tag{29}$$

subject to the stability conditions in Corollary 1.

It is noted that the tasks of swing-up and balance can be achieved with the minimization of designated fitness functions. By observation, minimizing the value of the fitness function (28) means that the system energy is increased, i.e. the system energy can be accumulated. Also, if pendulum and cart are stabilized at the designated equilibrium positions, the fitness value of (29) is identically to zero.

Table 2. System parameters of pendulum-cart system.

Parameter	Value	Unit	Parameter	Value	Unit
f_p	21x10^{-66}	Kgm^2/s	V_{DZ}	0.08	*m/s*
g	9.81	m^2/s	m_p	0.095	*Kg*
F_s	3.2	*N*	m_c	1.12	*Kg*
F_c	2.3	Kg/s	l	0.01407	*m*
X_c	2.5	*m/s*	J	0.003863	Kgm^2
Y_c	2.5	*N*			

The initial states of the pendulum-cart system are set to be $x = [0 \quad \pi \quad 0 \quad 0]$ and the disturbance is added at 10 sec. Fig. 10(a) indicates the responses of the pendulum-cart system with hybrid fuzzy controllers without PSO. The responses of the pendulum-cart system using the RT-PSO optimized fuzzy controllers are shown in Fig. 10(b). It can be seen that, from Fig.10(a), before 10 sec, the pendulum is swung up and balanced upright as desired and the cart is also at the required position. However, after the disturbance added at 10 sec, the hybrid fuzzy controllers without PSO can never be affordable for dynamic changes and fails to bring the pendulum back to the balance zone due to extra accumulated energy. However, in Fig. 10(b), the hybrid fuzzy controllers with RT-PSO performs well, and the desired goals, $x_1 = 0$ and $x_2 = 0$, are preserved subject to added disturbance.

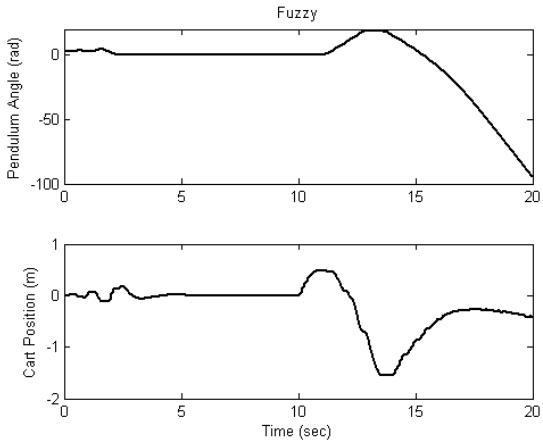

(a)

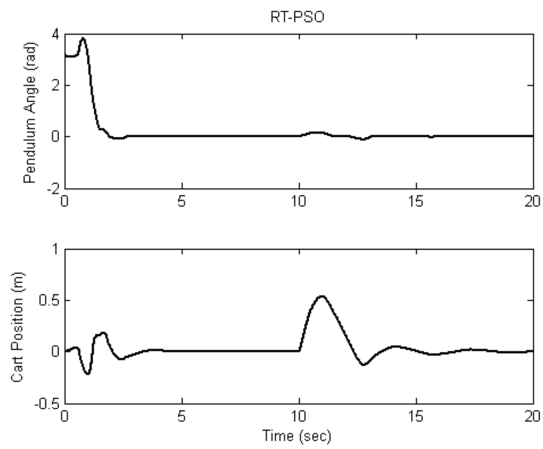

(b)

Fig. 10. Controlled responses of the pendulum-cart system. (a) conventional fuzzy control, (b) RT-PSO fuzzy control.

Fig. 11(b) presents the RT-PSO tuning responses of the parameters S_{u1}, S_{u2}, and S_{u3} of the output membership functions in the FSC. It can be observed that the updating process is stopped while the system is in the balance zone. Similarly, the tuning responses of the parameters P_{u1} and P_{u2} of the output membership functions for the FPBC, are shown in Fig. 11(a). For the parameter tuning of the FCBC, the values of C_{u1} and C_{u2} are also indicated in Fig. 11(a), respectively. It can be seen that the parameter adjustment becomes significant for FPBC and FCBC while the disturbance is added. From simulation results, the satisfactory responses as expected are achieved to have the pendulum and cart stabilized at their equilibrium points, $x_1 = 0$, $x_2 = 0$.

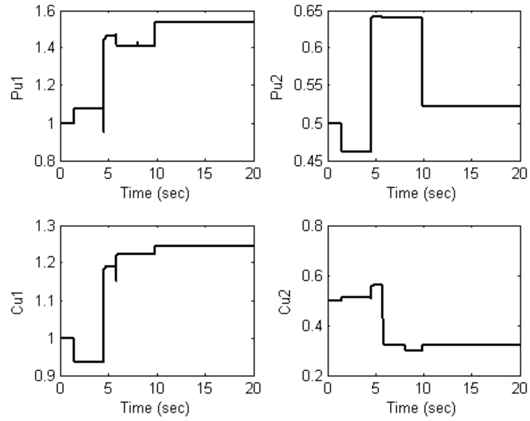

(a)

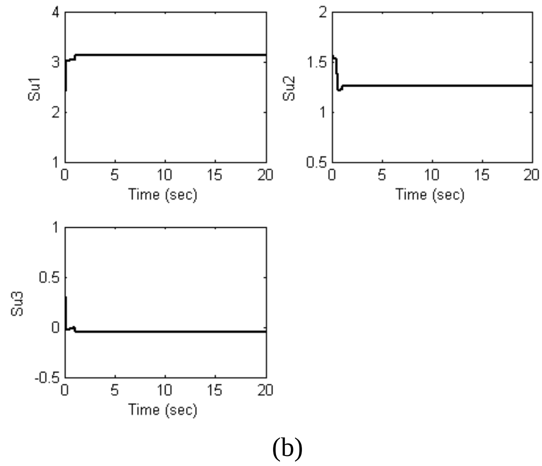

(b)

Fig. 11. Parameters tuning via RT-PSO. (a) parameters of FPBC and FCBC, (b) parameters of FSC.

6. Conclusion

This paper presents a hybrid fuzzy controller with a real-time PSO algorithm for a pendulum-cart system. The proposed RT-PSO has the desired capability to monitor the dynamical environments and re-start the random searching subject to the environmental variations. The feasibility of the RT-PSO algorithm is also evaluated by a dynamic test function. For the hybrid fuzzy control of a pendulum-cart system, the proposed RT-PSO is applied to optimize the parameter settings of the output membership functions. LMI stability conditions are derived to ensure the closed-loop stability of the fuzzy control system. Simulation results illustrate that the RT-PSO optimized fuzzy controller can provide better control performance subject to disturbance.

References

[1] A. Chatterjee, K. Pulasinghe, K. Watanabe, and K. Izumi, "A particle-swarm-optimized fuzzy-neural network for voice-controlled robot systems," *IEEE Trans. on Industrial Electronics*, vol. 52, no. 6, pp 1478-1489, 2005.

[2] A. Ratnaweera, S. Halgamuge, and H. C. Watson, "Self-organizing hierarchical particle swarm optimizer with time-varying acceleration coefficients," *IEEE Trans. on Evol. Comput*., vol. 8, no. 3, pp. 240-255, 2004.

[3] Y. del Valle, G. K. Venayagamoorthy, S. Mohagheghi, J.-C. Hernandez, and R. G. Harley, "Particle swarm optimization: basic concepts, variants and applications in power systems," *IEEE Trans. on Evol. Comput*., vol. 12, no. 2, pp.171-195, 2008.

[4] J. Robinson and Y. Rahmat-Samii, "Particle swarm optimization in electromagnetics," *IEEE Trans. on Antennas and Propagatio*n, vol. 52, no. 2, pp. 397-407, 2004.

[5] Z. L. Gaing, "A particle swarm optimization approach for optimum design of PID controller in AVR system," *IEEE Trans. on Energy Conversion*, vol. 19, no. 2, pp. 384-391, 2004.

[6] M. R. AlRashidi and M. E El-Hawary, "A survey of particle swarm optimization applications in electric power systems," *Electric Power Components and Systems*, vol. 34, no. 12, pp. 1349-1352, 2008.

[7] S. P. Ghoshal, "Optimizations of PID gains by particle swarm optimizations in fuzzy based automatic generation control," *Electric Power Systems Research*, vol. 72, pp. 203-212, 2004.

[8] S. Patchararungruang, S. K. Halgamuge, and N. Shenoy, "Optimized rule-based delay proportion adjustment for proportional differentiated services," *IEEE Journal on Selected Areas in Communications*, vol. 23, no. 2, pp. 261-276, 2005.

[9] C. F. Juang and C. H. Hsu, "Temperature control by chip-implemented adaptive recurrent fuzzy controller designed by evolutionary algorithm," *IEEE Trans. on Circuits and systems I: Regular Papers*, vol. 52, no. 11, pp. 2376-2384, 2005.

[10] H. M. Feng, "Self-generation RBFNs using evolutional PSO learning," *Neurocomputing*, vol. 70, pp. 241-251, 2006.

[11] T. Huang and A. S. Mohan, "A hybrid boundary condition for robust particle swarm optimization," *IEEE Antennas and Wireless Propagation Letters*, vol. 4, no. 1, pp. 112-117, 2005.

[12] W. Liu, E. McGrath, C.-C. Hung, and B.-C. Kuo, "Hybridization of particle swarm optimization with unsupervised Clustering Algorithms for Image Segmentation," *International Journal of Fuzzy Systems*, vol. 10, no. 3, pp. 217-230, 2008.

[13] D. Parrott and X. Li, "Locating and tracking multiple dynamic optima by a particle swarm model using speciation," *IEEE Trans. on Evol. Comput*., vol. 10, no. 4, pp. 440-458, 2006.

[14] T. Blackwell and J. Branke, "Multiswarms, exclusion, and anti-convergence in dynamic environments," *IEEE Trans. on Evol. Comput*., vol. 10, no. 4, pp. 459-472, 2006.

[15] D. Chatterjee, A. Patra, and H. K. Joglekar, "Swing-up and stabilization of a cart-pendulum system under restricted cart track length," Systems *and Control Letters*, vol. 47, no. 4, pp. 355-364, 2002.

[16] K. Tanaka and H. O. Wang, *Fuzzy control systems design and analysis*, Upper Saddle River, NJ: Prentice-Hall, 2001.

[17] C. W. Tao, J. S. Taur, W. H. Tzuen, and C. L. Tsai, "Design of a fuzzy controller with fuzzy swing-up and parallel distributed pole assignment schemes for an inverted pendulum and cart system," *IEEE Tran. on Control System Technology*, vol. 16, no. 6, pp. 1277-1288, 2008.

[18] W. Y. Wang, Y. H. Chien, and I.H. Li, "An On-Line Robust and Adaptive T-S Fuzzy-Neural Controller for More General Unknown Systems," *International Journal of Fuzzy Systems*, Vol. 10, No. 1, pp. 33-43, March 2008.

[19] C.-W. Tao, J.-S. Taur, J.-T. Jeng, and W.-Y. Wang, "A Novel Fuzzy Ant Colony System for Parameter Determination of Fuzzy Controllers," *International Journal of Fuzzy Systems*, Vol. 11, No. 4, pp. 298-307, December 2009.

Yeong-Hwa Chang received the B.S. degree in electrical engineering from the Chung Cheng Institute of Technology, Tao-Yuan, Taiwan, the M.S. degree in control engineering from the National Chiao Tung University, Hsin-Chu, Taiwan, and the Ph.D. degree in electrical engineering from the University of Texas at Austin, U.S.A., in 1982, 1987, and 1995, respectively. He is currently an Associate Professor with the Department of Electrical Engineering, Chang Gung University, Tao-Yuan, Taiwan, R.O.C. His research interests include intelligent systems, haptics, and swarm robots.

Chia-Wen Chang received the B.S. degree in electrical engineering from National I-Lan Institute of Technology, I-Lan, Taiwan, R.O.C., in 2001, and the M.S. degrees in electrical engineering from Chang Gun University, Tao-Yuan, Taiwan, R.O.C., in 2003, where he is currently pursuing the Ph.D. degree in intelligent control. His current research interests are on the intelligent control systems including fuzzy control systems and swarm intelligent optimization.

Wei-Shou Chan received the B.S. degree in electrical engineering from Lung Hwa University of Science and Technology, Tao-Yuan, Taiwan, R.O.C., in 2003, and the M.S. degrees in electrical engineering from Chang Gung University, Tao-Yuan, Taiwan, R.O.C., in 2006, where he is currently pursuing the Ph.D. degree in intelligent control. His current research interests are on the nonlinear control and fuzzy control.

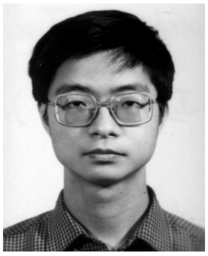

Jinshiuh Taur received his B.S. and M.S. degrees in Electrical Engineering from National Taiwan University, Taipei, Taiwan, R.O.C., in 1987 and 1989, respectively, and his Ph.D. degree in Electrical Engineering from Princeton University, in 1993. He was a Member of Technical Staff in Siemens Corporate Research, Inc. He is currently a Professor at the National Chung-Hsing University in Taiwan. His primary research interests include neural networks, pattern recognition, computer vision, and fuzzy logic systems.

C. W. Tao received the B.S. degree in electrical engineering from National Tsing Hua University, Hsinchu, Taiwan, R.O.C., in 1984, and the M.S. and Ph.D. degrees in electrical engineering from New Mexico State University, Las Cruces, in 1989 and 1992, respectively.

He is currently a Professor with the Department of Electrical Engineering, National I-Lan University, I-Lan, Taiwan, R.O.C.. He is an Associate Editor of the IEEE Transactions on Systems, Man, and Cybernetics. His research interests are on the fuzzy neural systems including fuzzy control systems and fuzzy neural image processing.

Dr. Tao is an IEEE Senior Member.